Kilometer-precise (UII) Umbriel physical properties from the multichord stellar occultation on 2020 September 21

Marcelo Assafin
Federal University of Rio de Janeiro, Valongo Observatory, Brazil

S. Santos-Filho, B, E. Morgado, A. R. Gomes-Júnior, B. Sicardy, G. Margoti,G. Benedetti-Rossi, F. Braga-Ribas, T. Laidler, J. I. B. Camargo, R. Vieira-Martins, T. Swift, D. Dunham, T. George, J. Bardecker, C. Anderson, R. Nolthenius, K. Bender, G. Viscome, D. Oesper, R. Dunford, K. Getrost, C. Kitting, K. Green, R. Bria, A. Olsen, A. Scheck, B. Billard, M. E. Wasiuta, R. Tatum, P. Maley, D. di Cicco, D. Gamble, P. Ceravolo, D. Ceravolo, W. Hanna, N. Smith, N. Carlson, S. Messner, J. Bean, J. Moore and R. Venable

Presentation topics

- Scientific context
- Observations
- Photometry
- Ingress and egress occultation instants
- Limb fittings
- Results: shape, size, density, albedo, position, …
- Atmosphere limits
- Umbriel strong variation of limb on both hemispheres

- Uranus and Neptune-type ice giants may be typical representatives of a common class of exoplanets, yet they are the least explored planets in the Solar System (only 1 flyby in 1986 by Voyager 2, which observed the southern hemisphere of the planets and moons)
- Uranus is a rich system and good laboratory for Planetology: 5 moons, 13 moonlets, complex ring system, …
- Main moons' surfaces are formed of H_2O ice, carbon-based ices including CO_2 and nitrogen-based ices such as NH_3 (recent geological activity?)
- Moons' true constituents (oceans?) are not known
- A launch window opportunity will occur in 2030–2034 due to a favorable gravity assist configuration by Jupiter, allowing a probe to reach the system before its 2050 equinox, after which the northern hemisphere will again become inaccessible (space missions are now being proposed/investigated)
- Comparison between the currently visible northern hemisphere with southern hemisphere results by Voyager 2 is essential to guide the investigations by such space missions.
- In this context, a successful campaign was carried out in 21 September 2020 at the USA and Canada for the observation of a stellar occultation by Umbriel with 19 positive chords

Occulted star	
Epoch	2020-09-21 08:24:36.000 UTC
Source ID	Gaia DR3 75195604519240064
Star position (1)	$\alpha = 02^h\ 30^m\ 28.^s84657 \pm 0.0873$ mas
	$\delta = 14^o\ 19'\ 36''.3762 \pm 0.0860$ mas
Magnitudes (2)	R = 13.474 ± 0.002; G = 13.779 ± 0.002
	B = 14.183 ± 0.002; J = 11.904 ± 0.021
	H = 11.412 ±0.023; K = 11.323 ± 0.022
	Absolute G magnitude = 3.214443
RUWE (3)	1.11
Apparent diameter (4)	0.0246 mas = 0.339 km
Star class (5)	Main sequence dwarf or sub-giant G-type star

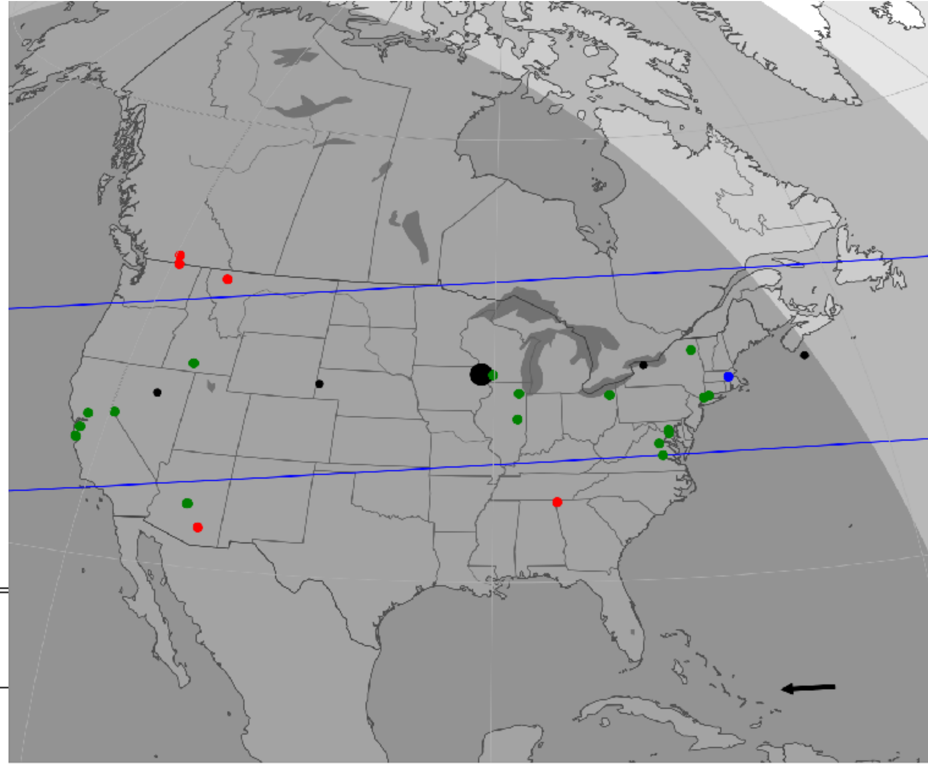

Observer	Latitude (o ′ ″), Longitude (o ′ ″), Altitude (m)	D(cm), f/, Detector, Format	Observation (UTC) Start (08:mm:ss), End (08:mm:ss)	Exp. time (s), Cycle time (s), Time device	Status
Dave Gamble, CAN	+49 35 34.000, -119 41 55.900, 522	45.70, 04.5, 1, FITS	19:00 - 29:00	0.11300, 0.11300, GPS	N
Peter Debra Ceravolo, CAN	+49 00 32.000, -119 21 47.000, 1097	28.00, 05.0, 1, FITS	24:00 - 28:00	0.35000, 0.35141, GPS	N
Willian Hanna, USA	+48 23 38.730, -114 12 43.960, 979	27.94, 10.0, 1, FITS	21:37 - 30:03	1.00000, 1.00235, GPS	N
Chris Anderson, USA	+42 35 01.800, -114 28 13.200, 1120	60.00, 12.8, 4, AVI	22:48 - 30:15	2.06832, 2.06930, GPS	P
Steve Messner, USA	+44 29 57.500, -093 07 45.080, 289	45.00, 03.0, 3			O
George Viscome, USA	+44 15 40.140, -074 00 25.460, 596	36.83, 06.0, 2, FITS	19:31 - 25:38	0.17500, 0.17630, GPS	P
David Oesper, USA	+42 57 36.900, -090 08 31.100, 390	30.50, 03.3, 3, AVI	09:00 - 36:10	0.12800, 0.13310, GPS	P
James Bean, USA					O
Dennis diCicco, USA	+42 21 01.000, -071 23 21.000, 43	40.60, 20.0, 5	20:01 - 28:00	0.25000, 0.25000, NTP	L
Jerry Bardecker, USA	+38 53 23.500, -119 40 20.300, 1524	30.48, 10.0, 3, AVI	23:15 - 29:30	0.03330, 0.03330, GPS	P
Ted Swift, USA	+38 33 08.260, -121 47 08.140, 18	20.00, 10.0, 3, AVI	24:30 - 28:30	0.26400, 0.26700, GPS	P
Robert Dunford, USA	+41 45 32.400, -088 07 00.010, 230	35.56, 01.9, 1, FITS	18:52 - 28:46	3.00000, 3.00070, GPS	P
Kai Getrost, USA	+41 35 06.100, -081 04 45.720, 348	25.40, 10.0, 1, FITS	20:01 - 28:06	0.50000, 0.50030, GPS	P
Chris Kitting, USA	+37 38 48.840, -122 02 09.096, 189	25.40, 04.7, 3, AVI	23:00 - 30:30	0.26640, 0.26670, GPS	P
Kevin Green, USA	+41 10 15.900, -073 19 39.300, 87	35.60, 07.7, 1, SER	18:39 - 27:18	1.00000, 1.00220, GPS	P
Rick Bria, USA	+41 04 01.000, -073 41 30.000, 118	35.50, 07.2, 3, AVI	20:00 - 26:05	0.13320, 0.13320, GPS	P
Kirk Bender, USA	+37 03 27.470, -122 07 23.200, 555	20.32, 10.0, 3, AVI	23:30 - 31:00	0.26640, 0.26700, GPS	P
Richard Nolthenius, USA	+37 01 04.120, -122 04 45.310, 341	20.32, 06.3, 3, AVI	23:10 - 30:00	0.52800, 0.53390, GPS	P
Aart Olsen, USA	+40 05 12.400, -088 11 46.300, 224	50.00, 04.0, 6, AVI	19:27 - 29:27	0.40000, 0.40000, GPS	P
Andrew Scheck, USA	+39 08 59.070, -076 53 13.330, 120	20.00, 06.3, 7, MOV	20:36 - 24:51	0.99000, 1.00050, GPS	P
David Dunham, USA	+38 59 12.745, -076 52 08.880, 46	41.00, 04.4, 1, FITS	20:01 - 25:04	1.00000, 1.00050, GPS	P
Barton Billard & Myron E. Wasiuta, USA	+38 20 02.000, -077 42 38.000, 96	10.20, 07.0, 1, FITS	20:51 - 26:51	4.00000, 4.00172, GPS	P
John Moore, USA					T
Randy Tatum, USA	+37 35 42.576, -077 33 02.484, 77	30.00, 10.0, 8, AVI	21:22 - 26:16	0.10000, 0.10000, NTP	P
Paul Maley, USA	+33 48 42.858, -111 57 07.974, 654	28.00, 05.0, 3, AVI	24:57 - 27:55	0.53280, 0.53390, GPS	P
Tony George, USA	+33 49 00.100, -111 52 07.300, 843	30.00, 03.3, 3, AVI	24:30 - 28:30	0.13320, 0.13390, GPS	P
Ned Smith, USA	+34 52 30.000, -085 28 15.600, 210	63.50, 03.2, 1, FITS	20:14 - 28:13	1.00000, 1.00011, GPS	N
Normam Carlson, USA	+32 25 53.140, -110 44 43.940, 2391	23.50, 00.5, 9 AVI	23:28 - 30:00	0.13340, 0.13340, NTP	N
Roger Venable, USA					O

Notes. D(cm) = diameter. f/ = focal ratio. Status: P = positive, N = negative, L = video recording lost, T = technical problems, O = overcast. Detectors: 1 = QHY 174, 2 = QHY 174M, 3 = Watec 910HX, 4 = Watec 120N+, 5 = Celestron Skyris 618M, 6 = Watec 910BD, 7 = Mallincam, 8 = ZWO ASI224MC, 9 = RunCam Night Eagle Astro. Chords ordered from north to south in the sky plane.

Umbriel	
Ephemeris (6)	DE435/URA111
Geocentric distance	19.0194591323518 au
Apparent velocity	17.2 km s^{-1} (relative velocity Umbriel - star)
Apparent magnitude (7)	V = 14.978
Mass (8)	$(1.275 \pm 0.028) \times 10^{21}$ kg
Rotation period (9)	4.144 days
Pole (10)	RA = $17^h\ 08^m\ 55.^s6624$
	Dec = $-15^o\ 02'\ 00''.809$
Position angle (11)	P = 145.082 deg
Aspect angle (12)	$\zeta = 38^o\ 16'\ 24''.82$ (north pole)
Sub-observer point (13)	Longitude = $204^o\ 20'\ 04''.518$
at Umbriel	Latitude = $+51^o\ 43'\ 35''.183$
Sub-Uranus point (14)	Longitude = $1^o\ 04'\ 17''.394$
at Umbriel	Latitude = $-0^o\ 11'\ 08''.356$

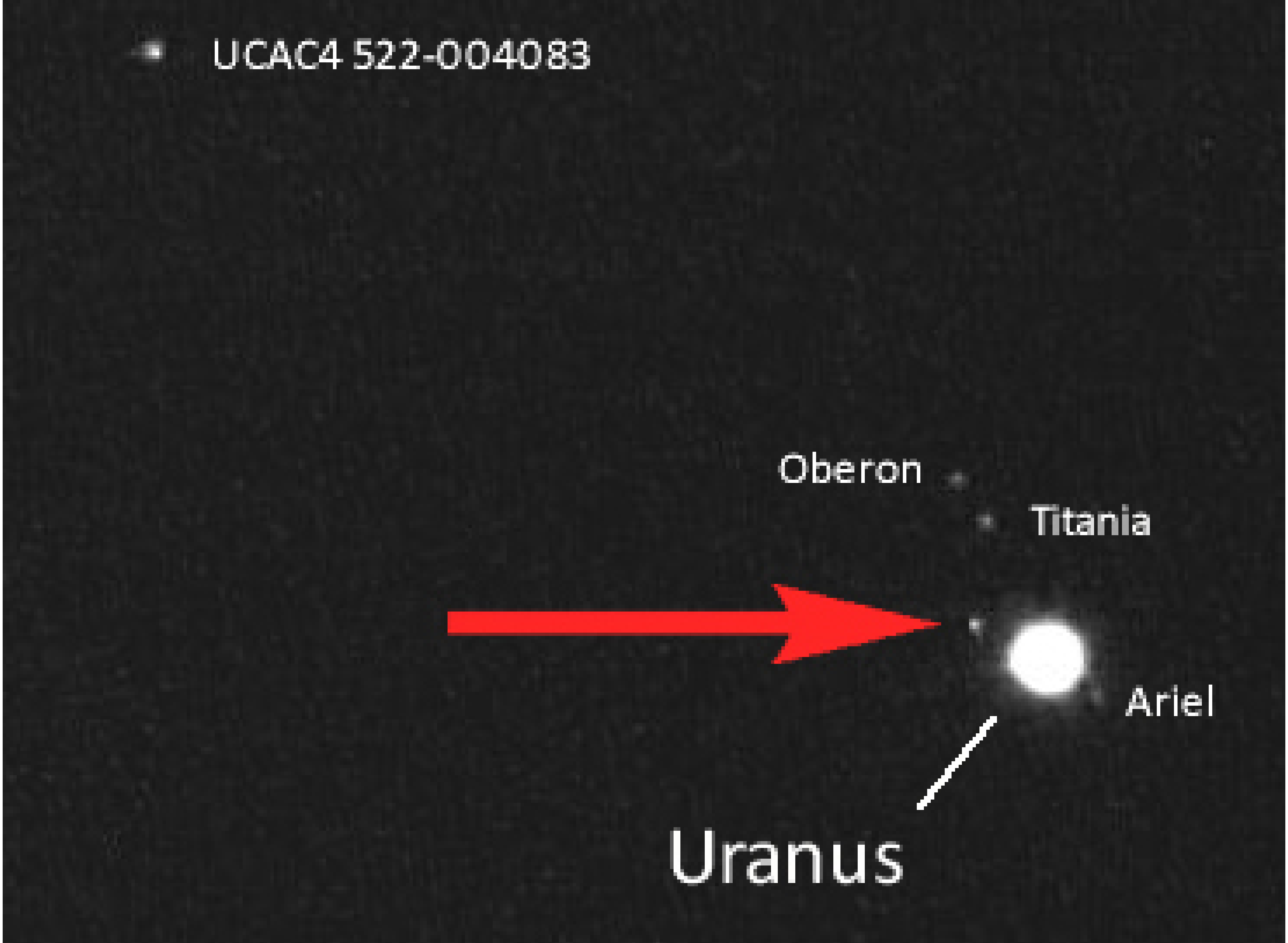
UCAC4 522-004083
Oberon
Titania
Ariel
Uranus

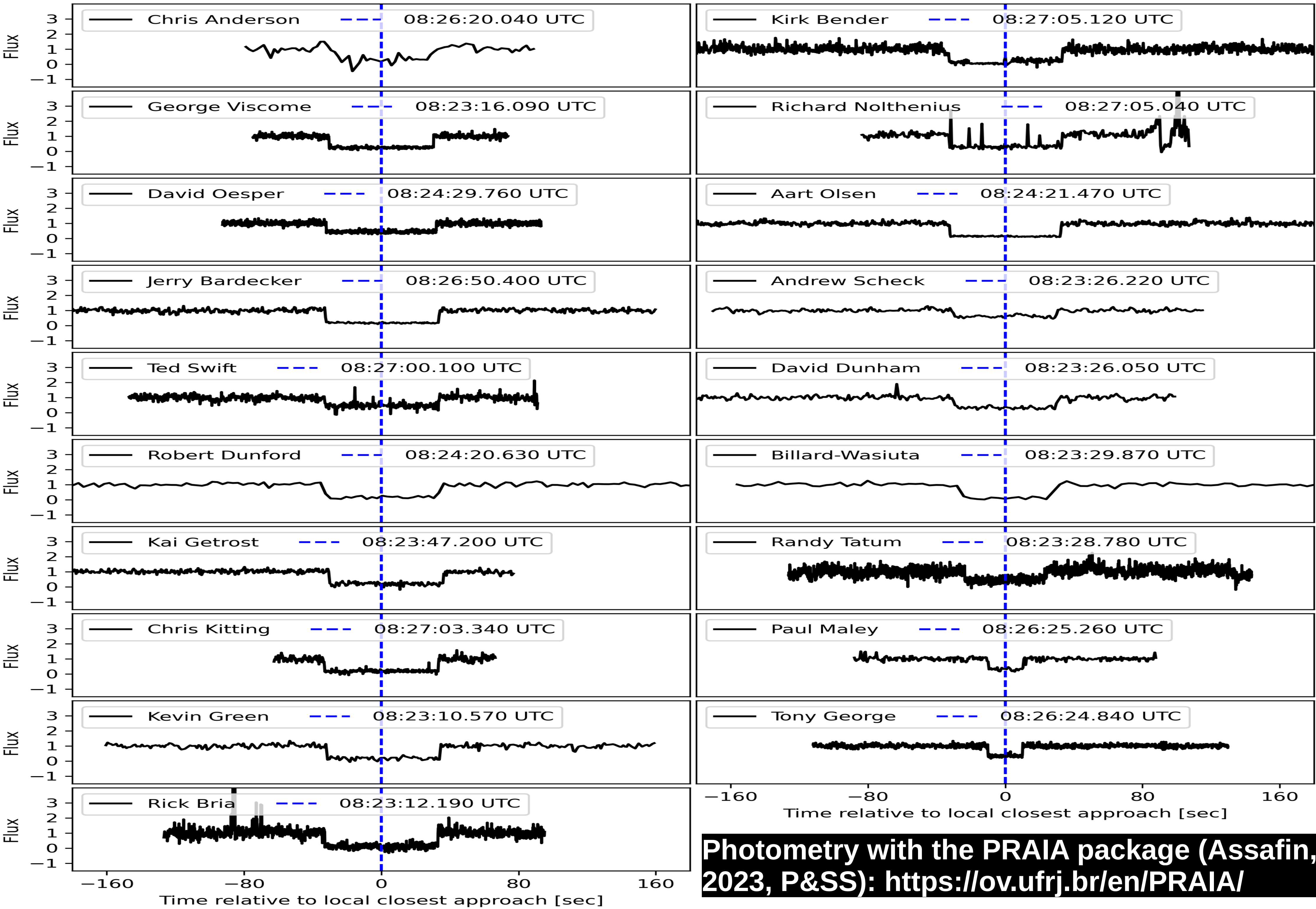

Photometry with the PRAIA package (Assafin, 2023, P&SS): https://ov.ufrj.br/en/PRAIA/

Ingress/egress instants: SORA package (Gomes-Júnior et al., 2022, MNRAS): https://github.com/riogroup/SORA

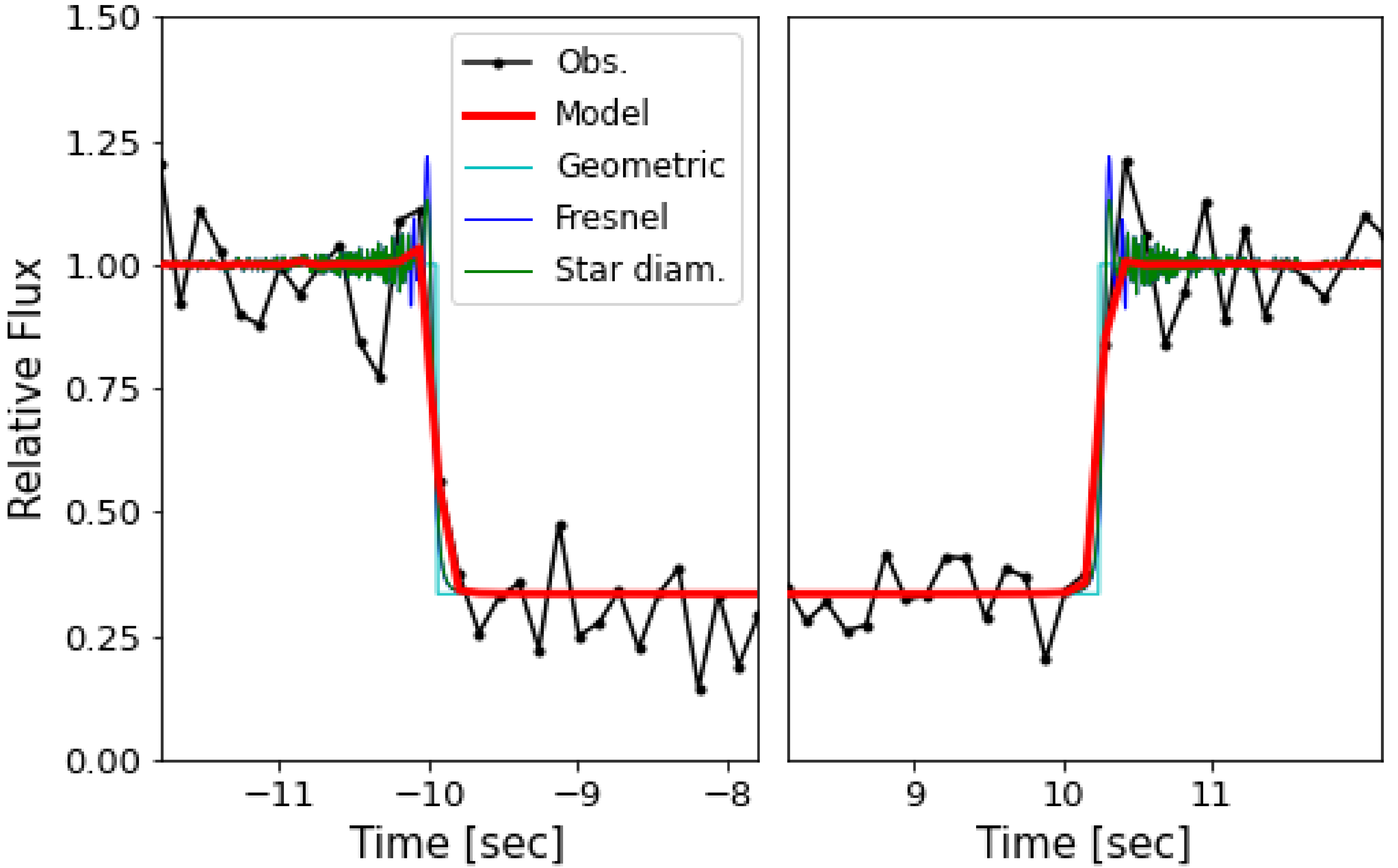

Observer	Ingress (08:mm:ss.s)	σ(s) σ(km)	Egress (08:mm:ss.s)	σ(s) σ(km)	Chord length (km)	(O-C)$_{IN}$ (km) Circle Ellipse	(O-C)$_{EG}$ (km) Circle Ellipse	σ (flux)	Coro Cal
Anderson	25:51.712	0.943	26:46.677	0.357	945.398 ± 17.343	+18.346 ± 16.439	-5.560 ± 6.225	0.13	N
		16.220		6.140		19.533	-5.722		N
Viscome	22:45.657	0.028	23:46.549	0.023	1047.342 ± 0.623	+3.662 ± 0.488	+4.105 ± 0.401	0.10	N
		0.482		0.396		+4.602	+3.940		C
Oesper	23:57.557	0.022	25:01.655	0.024	1102.486 ± 0.560	+1.833 ± 0.384	-3.412 ± 0.419	0.11	C
		0.378		0.413		+2.502	-3.489		C
Bardecker	26:17.330	0.066	27:23.519	0.069	1138.451 ± 1.642	-2.417 ± 1.151	-1.557 ± 1.203	0.11	C
		1.135		1.187		-2.034	-1.460		C
Swift	26:26.857	0.187	27:33.196	0.065	1141.031 ± 3.405	+0.217 ± 3.260	-2.140 ± 1.133	0.14	C
		3.216		1.118		+0.597	-2.040		C
Dunford	23:47.455	0.373	24:54.651	0.385	1155.771 ± 9.220	-2.138 ± 6.724	+12.690 ± 2.970	0.10	C
		6.416		6.622		-1.846	+12.852		C
Getrost	23:14.272	0.047	24:21.048	0.047	1148.547 ± 1.143	-7.269 ± 0.821	+8.724 ± 0.821	0.09	C
		0.808		0.808		-7.086	+8.976		C
Kitting	26:29.916	0.047	27:36.347	0.051	1142.613 ± 1.193	+0.923 ± 0.819	-6.404 ± 0.889	0.15	C
		0.808		0.877		+1.073	-6.113		C
Green	22:37.692	0.085	23:43.770	0.053	1136.542 ± 1.723	-5.969 ± 1.483	-0.355 ± 0.925	0.11	C
		1.462		0.912		-5.904	+0.010		C
Bria	22:39.130	0.031	23:45.047	0.038	1133.772 ± 0.844	-1.692 ± 0.541	-5.146 ± 0.663	0.18	C
		0.533		0.654		-1.650	-4.751		C
Bender	26:31.960	0.133	27:38.105	0.073	1137.694 ± 2.610	+1.211 ± 2.319	-1.633 ± 1.273	0.19	N
		2.288		1.256		+1.226	-1.198		C
Nolthenius	26:31.794	0.206	27:37.742	0.180	1134.306 ± 4.705	+3.326 ± 3.592	-5.914 ± 3.140	0.35	C
		3.543		3.096		+3.332	-5.464		C
Olsen	23:49.104	0.092	24:53.865	0.118	1113.889 ± 2.574	-1.102 ± 1.607	-0.412 ± 2.062	0.10	C
		1.582		2.030		-1.206	+0.170		C
Scheck	22:56.083	0.283	23:56.284	0.214	1035.457 ± 6.103	+3.751 ± 3.943	+2.744 ± 3.739	0.07	N
		4.868		3.681		+3.484	+3.660		C
Dunham	22:55.982	0.210	23:55.951	0.202	1031.467 ± 5.012	+10.195 ± 3.668	+7.622 ± 3.529	0.14	C
		3.612		3.474		+9.919	+8.576		C
Billard-Wasiuta	23:03.893	0.711	23:57.896	0.414	928.852 ± 14.151	-15.204 ± 12.424	+13.803 ± 7.235	0.08	C
		12.229		7.121		-15.484	+14.912		N
Tatum	23:05.211	0.030	23:51.710	0.033	799.783 ± 0.767	+2.691 ± 0.524	-5.068 ± 0.577	0.25	N
		0.516		0.568		+2.481	-3.785		C
Maley	26:14.879	0.073	26:35.260	0.099	350.553 ± 2.116	+0.606 ± 1.276	-1.399 ± 1.731	0.09	C
		1.256		1.703		+0.974	-0.163		C
George	26:14.606	0.018	26:34.791	0.020	347.182 ± 0.463	+0.461 ± 0.315	-1.078 ± 0.350	0.09	C
		0.310		0.344		+0.836	+0.156		C

Limb fittings: SORA package (Gomes-Júnior et al., 2022, MNRAS): https://github.com/riogroup/SORA

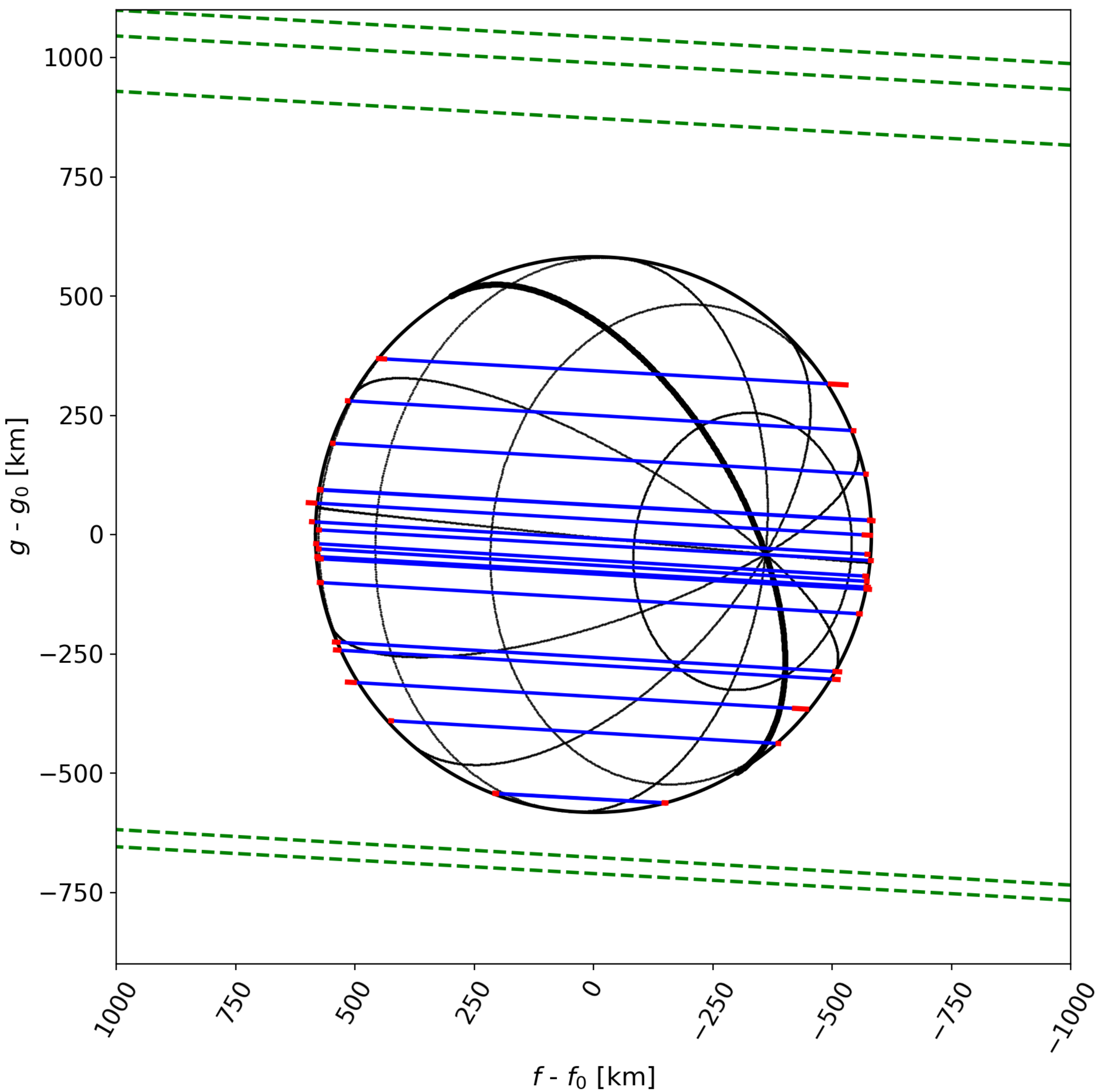

$$\chi^2 = \sum_{i=1}^{N} \frac{(r_{i,obs} - r_{i,cal})^2}{\sigma_i^2 + \sigma_{model}^2}$$

Circular limb	
Radius	$R = 582.4 \pm 0.8$ km (1-sigma)
Ephemeris offsets	$f_c = -23.7 \pm 0.8$ km
	$g_c = -169.4 \pm 1.9$ km
Limb parameter	$\sigma_{model} = 4.2$ km
χ^2 per degree of freedom	1.077
Elliptical limb	
Position angle [(1)]	P = 145.082 deg (fixed)
Apparent semi-major axis	$a' = 582.6 \pm 1.1$ km (1-sigma)
Apparent oblateness	$\epsilon' = 0.003 \pm 0.003$ (1-sigma)
Apparent equivalent radius [(2)]	$R'_{eq} = 581.7 \pm 2.0$ km
Ephemeris offsets (3)	$f_c = -23.7 \pm 0.9$ km
	$g_c = -169.5 \pm 2.0$ km
Limb parameter	$\sigma_{model} = 4.3$ km
χ^2 per degree of freedom	1.104

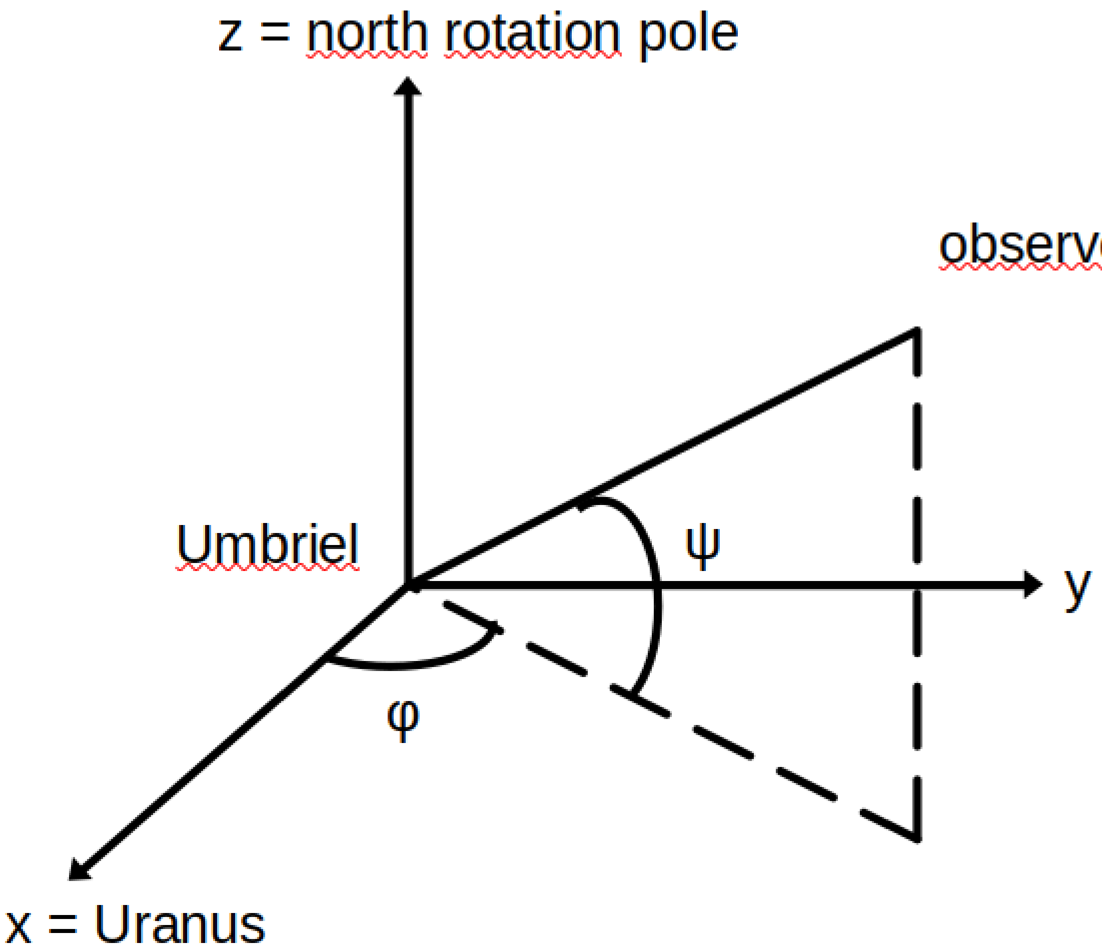

Apparent ellipse to true ellipsoid a > b = c

$$\frac{1}{a'^2} = \frac{r + s^{1/2}}{2\,t}\,, \quad \frac{1}{c'^2} = \frac{r - s^{1/2}}{2\,t}$$

$$r = (c^2 - a^2)\cos^2\psi\,\cos^2\varphi + a^2 + c^2$$

$$t = (c^4 - a^2c^2)\cos^2\psi\,\cos^2\varphi + a^2c^2$$

$$s = a^4(1 - \cos^2\psi\,\cos^2\varphi)^2 +$$
$$c^4\cos^2\psi(\cos^2\psi + 2\sin^2\psi\,\sin^2\varphi - 2\cos^2\varphi) +$$
$$2a^2c^2(\cos^4\psi\,\sin^2\varphi\,\cos^2\varphi - \sin^2\psi) +$$
$$2a^2c^2\cos^2\psi(\sin^2\psi\,\cos^2\varphi - \sin^2\varphi) +$$
$$c^4(1 - \cos^2\psi\,\sin^2\varphi)^2$$

Results

$$Volume = \frac{4\pi R^3}{3}$$

$$Density = \frac{mass}{volume}$$

$$Surface\ gravity = \frac{G\,M}{R^2}$$

$$Scape\ velocity = \sqrt{\frac{2\,G\,M}{R}}$$

$$Geometric\ albedo\ p = \left(\frac{au}{R}\right)^2 10^{0.4(H_{\odot} - H)}$$

$$(\alpha, \delta) \Leftarrow limb\ fitting$$

$$atmosphere\ limits \Leftarrow light\ curve\ fitting\ by\ atmosphere\ model\ using\ ray\ tracing$$

Umbriel physical characteristics from occultation	
Radius	$R = 582.4 \pm 0.8$ km
Limb parameter	$\sigma_{model} = 4.2$ km
Density (sphere)	$\rho = 1.54 \pm 0.04$ g cm^{-3}
Surface gravity	0.251 ± 0.006 m s^{-2}
Escape velocity	0.541 ± 0.006 km s^{-1}
Geometric albedo (sphere)	$p_V = 0.26 \pm 0.01$
Aspect angle	$\zeta = 38^o\ 16'\ 24''.82$ (north pole)
Isothermal CO_2 atmosphere	surface pressure = 13 – 72 nbar
at $T = 70$ K	(1–3σ upper limits)
Upper limits on putative Umbriel ellipsoid from occultation	
True semi-major axis	$a = 584.9 \pm 3.8$ km
True semi-minor axes	$b = c = 582.3 \pm 0.6$ km
True oblateness	$\epsilon = 0.004 \pm 0.008$
True equivalent radius [1]	$R_{eq} = 583.6 \pm 2.2$ km
Astrometry occultation data	
Ephemeris offsets [2]	$\Delta\alpha \cos\delta = -1.7 \pm 0.1$ mas
(mas)	$\Delta\delta = -12.3 \pm 0.2$ mas
Ephemeris offsets [2]	$\Delta\alpha \cos\delta = -23.7 \pm 0.8$ km
(km)	$\Delta\delta = -169.4 \pm 1.9$ km
Geocentric ICRS	$\alpha = 02^h\ 30^m\ 28.^s84556 \pm 0.1$ mas
position at epoch	$\delta = 14^o\ 19'\ 36''.5836 \pm 0.2$ mas
Reference occultation epoch	2020-09-21 08:24:36.000 UTC
Voyager II 1986 observations	
Radius (Voyager II, 1986)	$R = 584.7 \pm 2.8$ km (Thomas 1988)
Limb topography (Voyager II, 1986)	$\pm$ 5.0 km (Fig. 3 in Thomas 1988)
Aspect angle with the Sun [3]	$\zeta = 8^o$ (south pole)

Atmosphere limits

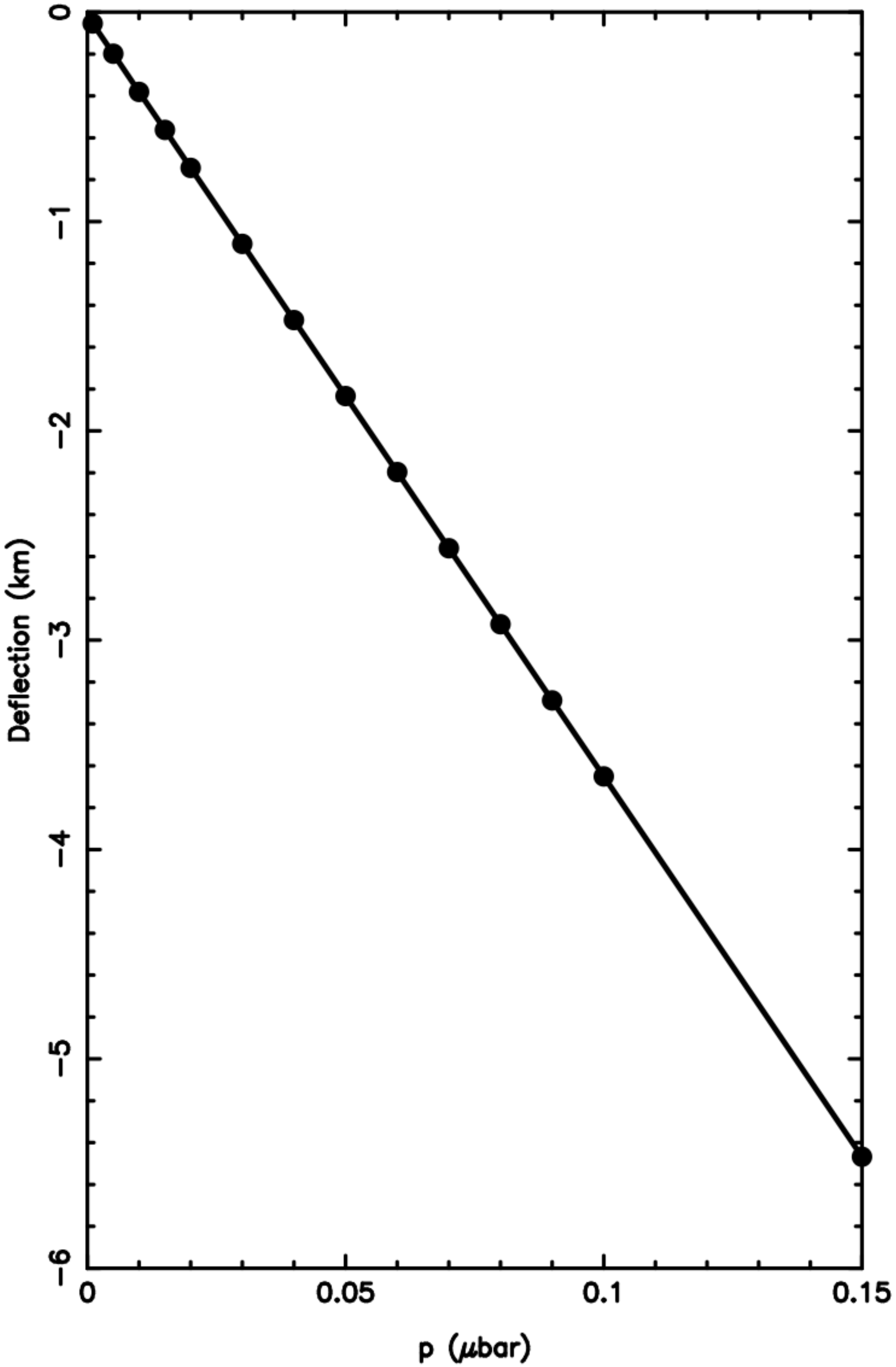

Isothermal CO_2 atmosphere at $T = 70$ K

$$R_{occ} - R_{V2} = -2.3 \pm 2.9\, km \Rightarrow 1\, \sigma\ upper\ limit < 5.2\, km$$

p = 150 nbar

Atmosphere limits

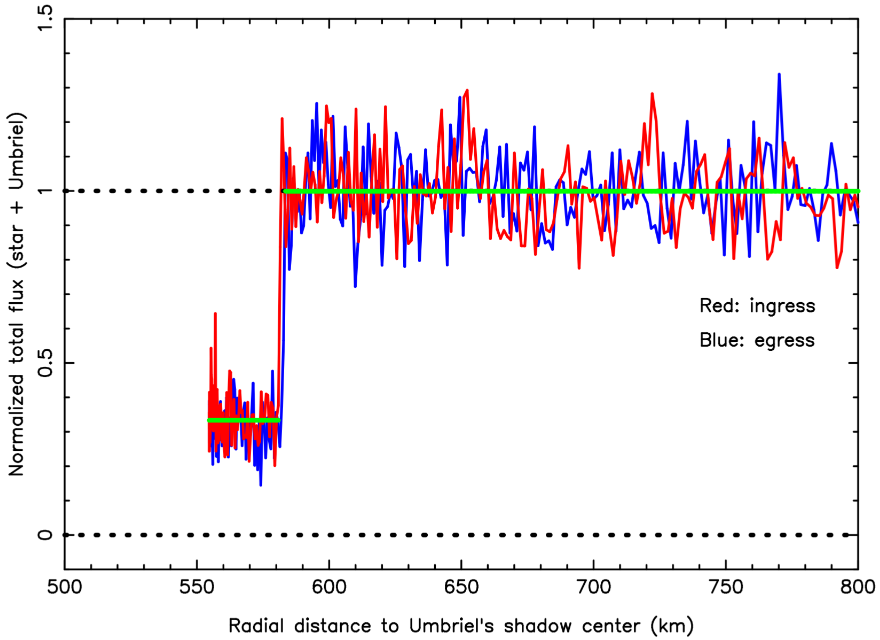

Isothermal CO_2 atmosphere
at T = 70 K

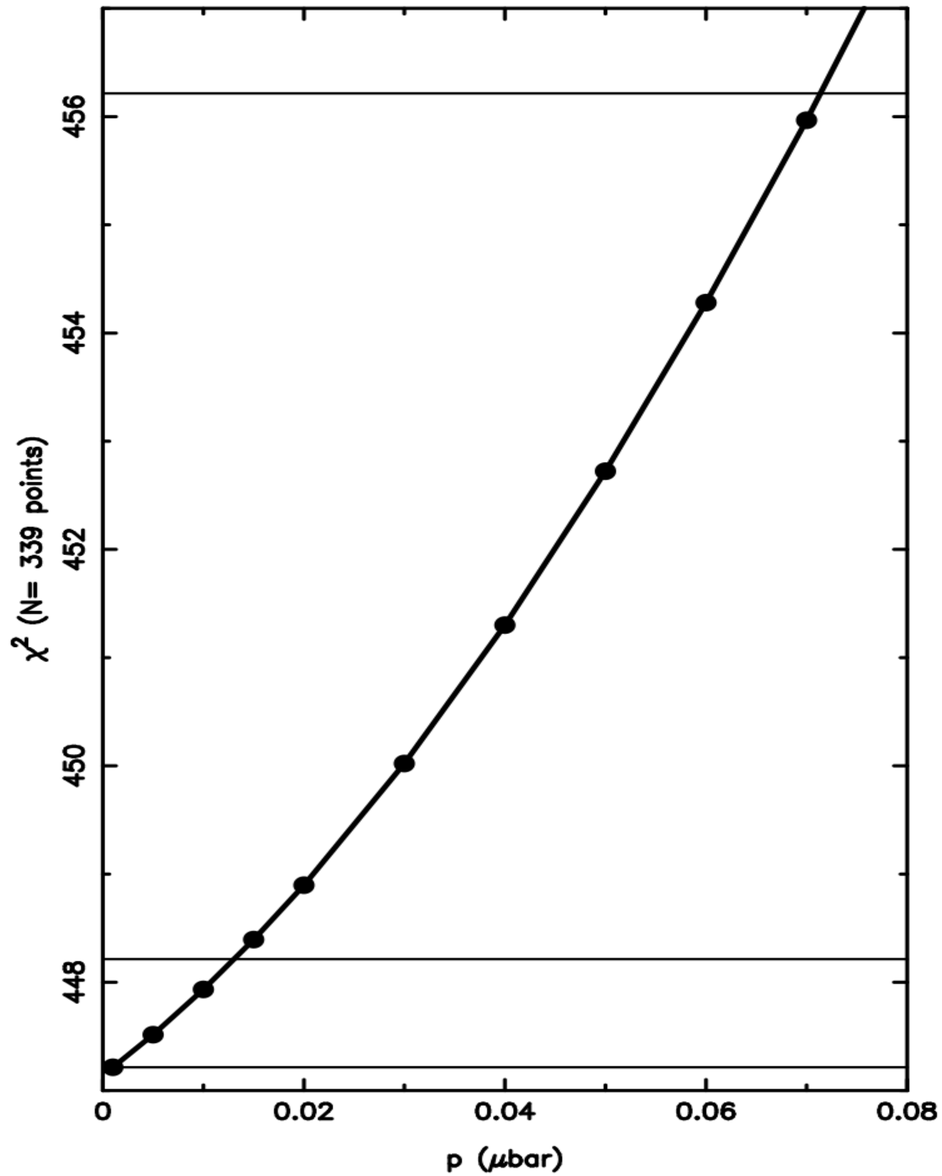

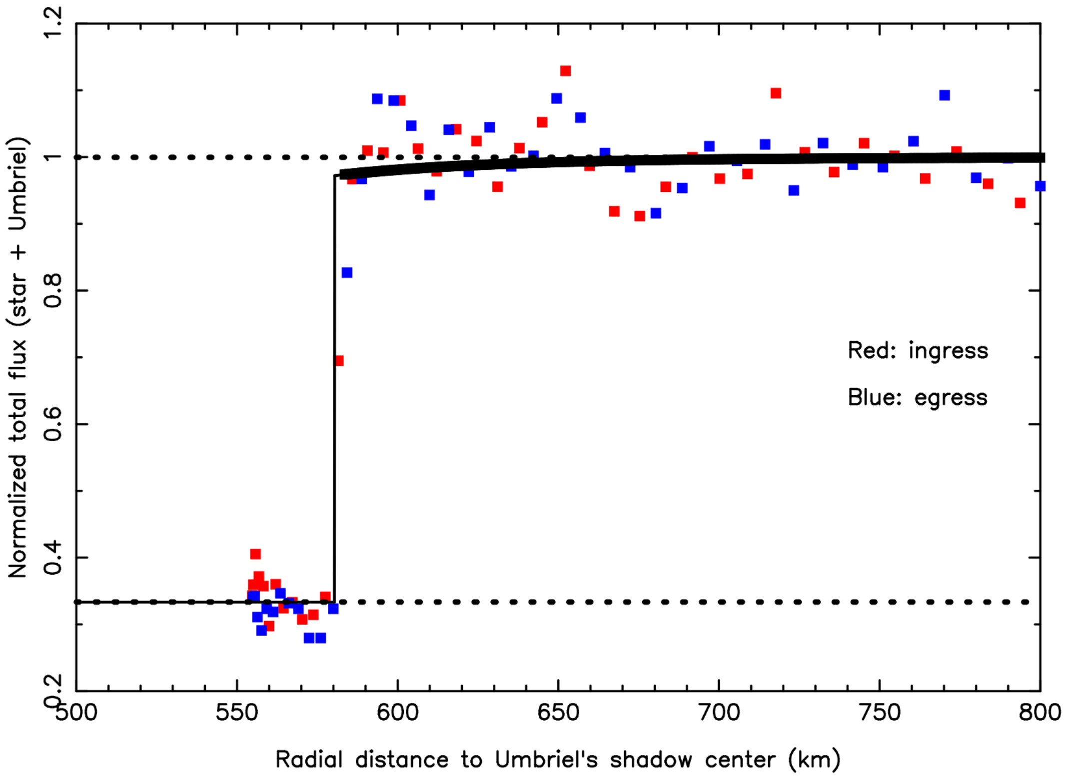

Isothermal CO_2 atmosphere
at T = 70 K

surface pressure = 13 – 72 nbar
(1–3 σ upper limits)

Umbriel strong limb variation at both hemispheres

Voyager 2 measurements of the southern hemisphere

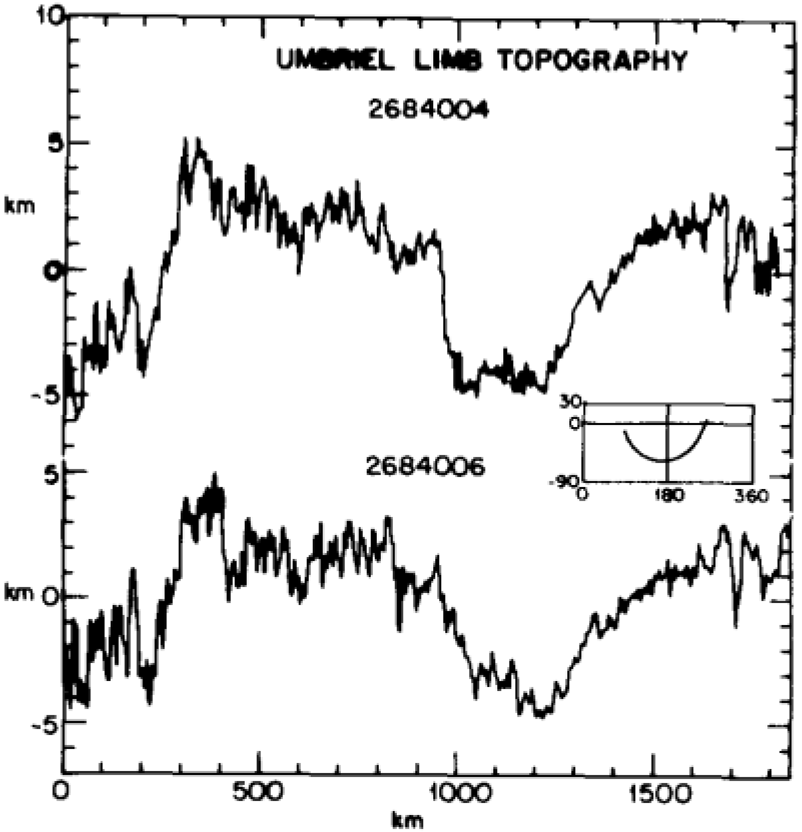

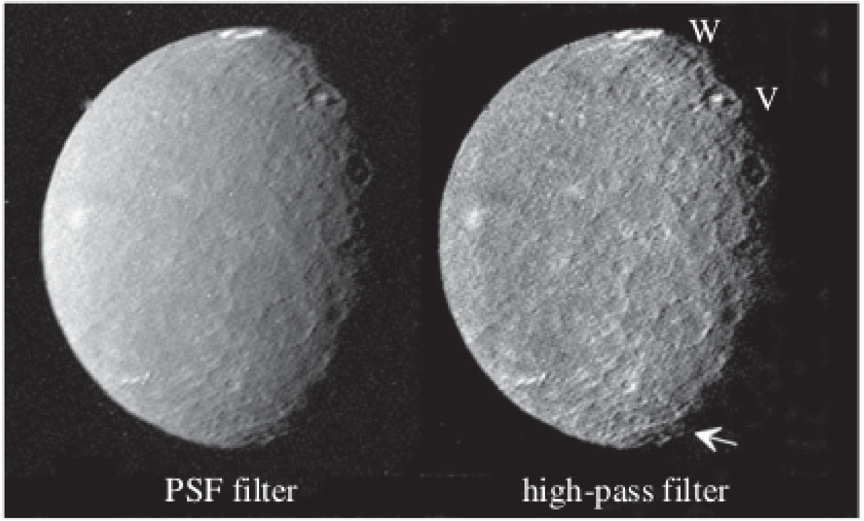

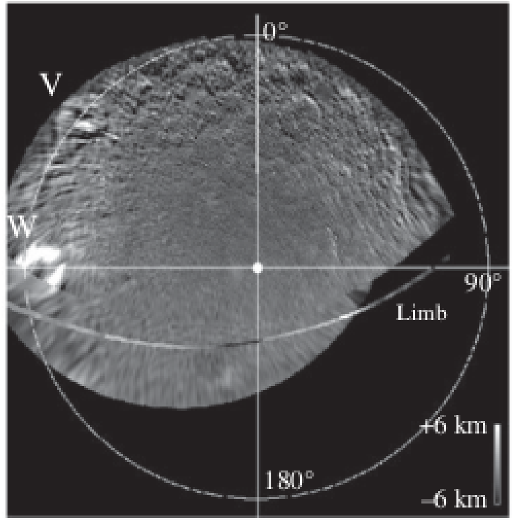

Left: P.C. Thomas (Ícarus 1988). Above: photoclinometry by P.M. Schenk & J.M. Moore (Philosophical Transactions A, 2020)

This occultation probed the northern hemisphere
==> Limb parameter = 4.2 km consistent with Voyager 2

Kilometer-precise (UII) Umbriel physical characteristics from the multichord stellar occultation on 2020 September 21

M. Assafin[1,2★], S. Santos-Filho[1,2,3], B, E. Morgado[1,2,9], A. R. Gomes-Júnior[5,2], B. Sicardy[6], G. Margoti[7,2], G. Benedetti-Rossi[8], F. Braga-Ribas[7,2], T. Laidler[1], J. I. B. Camargo[9,2], R. Vieira-Martins[9,2], T. Swift[10], D. Dunham[10], T. George[10], J. Bardecker[10], C. Anderson[11,10], R. Nolthenius[16,10], K. Bender[16], G. Viscome[12,10], D. Oesper[10], R. Dunford[10], K. Getrost[10], C. Kitting[13], K. Green[14,15], R. Bria[10], A. Olsen[10], A. Scheck[10], B. Billard[17,10], M. E. Wasiuta[17], R. Tatum[10], P. Maley[10], D. diCicco[10], D. Gamble[10], P. D. Ceravolo[10], W. Hanna[10], N. Smith[10,18], N. Carlson[10], S. Messner[10,19], J. Bean[10], J. Moore[10] and R. Venable[10]

[1]*Universidade Federal do Rio de Janeiro - Observatório do Valongo, Ladeira do Pedro Antonio 43, Rio de Janeiro, RJ 20.080-090, Brazil*
[2]*Laboratório Interinstitucional de e-Astronomia - LIneA and INCT do e-Universo, Rua Gal. José Cristino 77, Rio de Janeiro, RJ 20921-400, Brazil*
[3] *Universidade Federal do Rio de Janeiro - CEDERJ, R. Antonio Ferreira 110 – Rio da Areia – Bacaxá, Saquarema, RJ 28990-000, Brazil*
[4]*LESIA, Observatoire de Paris - Section Meudon, 5 Place Jules Janssen - 92195 Meudon Cedex, France*
[5]*Universidade Federal de Uberlândia (UFU), Instituto de Física, Av. João Naves de Ávila 2121, Bairro Santa Mônica, Uberlândia, MG 38408-100, Brazil*
[6]*LESIA, Observatoire de Paris, Université PSL, Sorbonne Université, Université de Paris, CNRS, 92190 Meudon, France*
[7]*Federal University of Technology - Paraná (PPGFA/UTFPR-Curitiba), Av. Sete de Setembro, 3165, Curitiba, PR 80230-901, Brazil*
[8]*Universidade Estadual de So Paulo (UNESP), Grupo de Dinâmica Orbital e Planetologia, Guaratinguetá, SP 12516-410, Brazil*
[9]*Observatório Nacional - MCTI, R. General José Cristino 77, Rio de Janeiro, RJ 20.921-400, Brazil*
[10]*International Occultation Timing Association (IOTA), PO Box 20313, Fountain Hills, AZ 85269, USA*
[11]*Centennial Observatory, Herrett Center for Arts & Science, College of Southern Idaho, Twin Falls, Idaho, USA*
[12]*Rand Observatory II - MPC W71, Lake Placid, NY, USA*
[13]*Biological Sciences, California State University, Hayward, CA 94542, USA*
[14]*University of New Haven, 300 Boston Post Road, West Haven, CT 06516, USA*
[15]*Westport Astronomical Society, 182 Bayberry Lane, Westport, CT 06880, USA*
[16]*Cabrillo College and Earth Futures Institute, UC Santa Cruz, 6500 Soquel Drive, Aptos, CA 95003, USA*
[17]*Mark Slade Remote Observatory, Wilderness, Virginia, USA*
[18]*Barnard Astronomical Society, Chattanooga, Hamilton County, Harrison Bay State Park, TN, USA*
[19]*Harvest Moon Observatory, H25, Northfield, MN, USA*

Accepted XXX. Received YYY; in original form 2023

ABSTRACT

We report the results of the stellar occultation by (UII) Umbriel on September 21st, 2020. The shadow crossed the USA and Canada, and 19 positive chords were obtained. A limb parameter accounted for putative topographic features in the limb fittings. Ellipse fittings were not robust. Only upper limits were derived for the true size/shape of a putative Umbriel ellipsoid. The adopted spherical solution gives radius = 582.4 ± 0.8 km, smaller/close to 584.7 ± 2.8 km from Voyager II. The obtained apparent semi-major axis of 582.6 ± 1.1 km and oblateness of 0.003 ± 0.003 result in a true semi-major axis of 584.9 ± 3.8 km, semi-minor axes of 582.3 ± 0.6 km and true oblateness of 0.004 ± 0.008 for a putative ellipsoid. The geometric albedo was p_V = 0.26 ± 0.01. A mass of (1.275 ± 0.028) × 10^{21} kg gives a density of ρ = 1.54 ± 0.04 g cm^{-3}. The surface gravity is 0.251 ± 0.006 m s^{-2} and the escape velocity 0.541 ± 0.006 km s^{-1}. Upper limits of 13 and 72 nbar (at 1σ and 3σ levels, respectively) were obtained for the surface pressure of a putative isothermal CO_2 atmosphere at T = 70 K. A milliarcsecond precision position was derived: $\alpha = 02^h\ 30^m\ 28.^s84556$ ± 0.1 mas, $\delta = 14^o\ 19'\ 36''.5836$ ± 0.2 mas. A large limb parameter of 4.2 km was obtained, in striking agreement with opposite southern hemisphere measurements by Voyager II in 1986. Occultation and Voyager results indicate that the same strong topography variation in the surface of Umbriel is present on both hemispheres.

Key words: planets and satellites: individual: (UII) Umbriel – occultations

THANKS !!